



# Quantitatively distinct requirements for signaling-competent cell spreading on engineered versus natural adhesion ligands

Gabriel P. Richman, David A. Tirrell, Anand R. Asthagiri\*

*Division of Chemistry and Chemical Engineering, California Institute of Technology, Mail Code 210-41, Pasadena, CA 91125, United States*

Received 24 June 2004; accepted 7 July 2004

Available online 12 October 2004

## Abstract

To design synthetic microenvironments that elicit desired cell behaviors, we must better understand the molecular mechanisms by which cells interact with candidate biomaterials. Using cell lines with distinct  $\alpha_5\beta_1$  integrin expression profiles, we demonstrate that this integrin mediates cell spreading on substrata coated with genetically engineered artificial extracellular matrix (aECM) proteins containing the RGD sequence (RGD-containing aECM protein [<sup>3</sup>RGD]) but lacking the PHSRN synergy site. Furthermore, <sup>3</sup>RGD-mediated adhesion stimulates an intracellular focal adhesion kinase (FAK) signal that is indicative of integrin tethering. Although both <sup>3</sup>RGD and the natural ECM protein fibronectin (FN) support  $\alpha_5\beta_1$  integrin-mediated cell spreading, quantitative single-cell analysis revealed that <sup>3</sup>RGD-mediated spreading requires ten-fold greater threshold amount of integrin expression than FN-mediated spreading. Our analysis demonstrates that <sup>3</sup>RGD-based substrata mediate both biophysical (cell spreading) and biochemical (FAK signaling) events via the  $\alpha_5\beta_1$  integrin, albeit with efficacy quantitatively distinct from that of natural ECM proteins that possess the full spectrum of adhesion and synergy domains.

© 2004 Elsevier B.V. All rights reserved.

**Keywords:** Biomaterial; Extracellular matrix; Focal adhesion kinase; Integrin; RGD

## 1. Introduction

Cell-adhesion ligands and their counterpart receptors differentially trigger downstream signals and

influence gene expression [1,2]. Thus, to begin to predict functional outcomes on any given biomaterial, gross confirmation of cell adhesion and spreading must be complemented by an understanding of the molecular mechanisms involved in cell–biomaterial interactions. This need is perhaps most evident for materials involving the RGD ligand, an effective promoter of cell attachment and spreading in several systems [3]. Part of its wide-ranging efficacy may be attributed to its broad specificity for numerous adhesion receptors, including  $\alpha_5\beta_1$  and  $\alpha_v\beta_3$  integrins [4]. Importantly, this specificity is context-

*Abbreviations:* aECM, artificial extracellular matrix; <sup>3</sup>RGD, RGD-containing aECM; <sup>3</sup>RDG, RDG-containing aECM; BSA, bovine serum albumin; CHO, Chinese hamster ovary; ECM, extracellular matrix; FN, fibronectin; GFP, green fluorescent protein; HUVEC, human umbilical vein endothelial cells.

\* Corresponding author. Tel.: +1 626 395 8130; fax +1 626 568 8743.

*E-mail address:* [anand@cheme.caltech.edu](mailto:anand@cheme.caltech.edu) (A.R. Asthagiri).

sensitive, since sequences near the RGD domain influence the type of integrins that are engaged [5,6]. For example, in certain cell types, a synergy site (PHSRN) is necessary for  $\alpha_5\beta_1$  but not  $\alpha_v\beta_3$  integrin engagement [7].

Indeed, such context dependence has been demonstrated for RGD-based artificial extracellular matrix (aECM) proteins ( $^a$ RGD, Fig. 1). Artificial extracellular matrix proteins are designed by intermixing domains from natural ECM proteins, such as fibronectin (FN) and elastin, to confer both cell adhesive and mechanical properties that are desirable for *in vivo* applications (Fig. 1) [8,9]. Human umbilical vein endothelial cells (HUVEC) adhere and spread on surfaces coated with  $^a$ RGD by employing focal adhesion complexes enriched with  $\alpha_v\beta_3$  integrins [8]. In contrast, HUVEC spread on FN-coated substrata with  $\alpha_5\beta_1$  integrin-rich focal adhesions. Importantly, in both cases, cell attachment is RGD-dependent, demonstrating context-specific utilization of integrins for RGD-dependent adhesion.

While these findings demonstrate the importance of  $\alpha_v\beta_3$  integrin in  $^a$ RGD-mediated HUVEC adhesion and spreading, they raise the important question whether this preference for  $\alpha_v\beta_3$  integrin is an endothelial cell-specific phenomenon or an innate property of RGD presented in the context of an aECM protein. This issue is particularly relevant for *in vivo* application since cell-material characterization offers only a glimpse of HUVEC behavior for an *ex vivo* “snapshot” of its integrin expression profile. *In vivo* integrin expression and the affinity/

avidity of integrin–ligand interactions are modulated dynamically by inside–out signaling [10]. Thus, in instances where the  $\alpha_v\beta_3$  integrin function in HUVEC is down-regulated, the competency of  $\alpha_5\beta_1$  integrin to bind  $^a$ RGD may determine how robustly this platform supports HUVEC attachment and spreading.

To study the competency of RGD to support  $\alpha_5\beta_1$  integrin-mediated cell spreading when presented in the context of an aECM protein, we engineered cell lines with well defined and, more importantly, distinct  $\alpha_5\beta_1$  integrin expression profiles. Chinese hamster ovary (CHO-B2) cells express minimal levels of  $\alpha_5\beta_1$  integrin and  $\beta_3$  integrins [11–14]. Starting from this reference cell line, we introduced exogenous  $\alpha_5$  integrin subunit by retroviral infection to generate an  $\alpha_5\beta_1$ -positive counterpart, thereby creating a pair of cell lines that could help to dissect the  $\alpha_5\beta_1$  integrin contribution to  $^a$ RGD-supported cell spreading.

## 2. Materials and methods

### 2.1. Cell culture

293T and CHO-B2 cells were gifts from D.V. Schaffer (University of California, Berkeley) and A.F. Horwitz (University of Virginia, Charlottesville), respectively. 293T cells were cultured in Dulbecco’s modified Eagle’s medium (Invitrogen, Carlsbad, CA) supplemented with 10% (v/v) fetal bovine serum (FBS) [Invitrogen Carlsbad, CA], 50 U ml<sup>-1</sup> penicillin

### $^a$ RGD

M-MASMTGGQMG-HHHHHHH-DDDDK(LD-YAVTGRGDSPASSKPIA((VPGIG)<sub>2</sub>VPGKG(VPGIG)<sub>2</sub>)<sub>4</sub>VP)<sub>3</sub>-LE

T7 tag	Histidine tag	Cleavage site	Cell-binding domain	Elastin-like repeat
--------	---------------	---------------	---------------------	---------------------

### $^a$ RDG

M-MASMTGGQMG-HHHHHHH-DDDDK(LD-YAVTGRDGSPASSKPIA((VPGIG)<sub>2</sub>VPGKG(VPGIG)<sub>2</sub>)<sub>4</sub>VP)<sub>3</sub>-LE

T7 tag	Histidine tag	Cleavage site	Scrambled cell-binding domain	Elastin-like repeat
--------	---------------	---------------	-------------------------------	---------------------

Fig. 1. Primary sequences of normal ( $^a$ RGD) and scrambled ( $^a$ RDG) aECM proteins used in this study. The artificial ECM proteins used in this work contain either the RGD cell-binding domain ( $^a$ RGD) or a scrambled counterpart ( $^a$ RDG). Elastin-like repeats were designed into the primary sequence so that protein gels composed of chemically cross-linked aECM proteins possess mechanical properties resembling those of natural elastin [19,20]. The other N-terminal sites denoted in the primary sequence assist in the synthesis and purification of these genetically engineered constructs.

and  $50 \mu\text{g ml}^{-1}$  streptomycin in a 5%  $\text{CO}_2$  humidified atmosphere. CHO-B2 cells were grown in similar medium, further supplemented with 1 mM of sodium pyruvate (Sigma-Aldrich, St. Louis, MO) and 1% (v/v) 100X non-essential amino acid solution (Sigma-Aldrich). Both cell lines were routinely passed with 0.05% trypsin in 0.53 mM EDTA (Invitrogen).

## 2.2. Retrovirus production and infection

293T cells were triple transfected with a retroviral expression vector (pLPCX or pLPCX- $\alpha_5$ -GFP) and plasmids encoding gag-pol (pCMV-gag-pol) and vesicular stomatitis virus glycoprotein (pCMV-VSVG) using lipofectamine (Invitrogen) according to manufacturer's specifications. Forty-eight hours after transfection, conditioned medium containing retrovirus was collected and passed through a  $0.45\text{-}\mu\text{m}$  syringe filter. For retroviral infection,  $2.5 \times 10^5$  CHO-B2 cells were treated with retrovirus-containing medium supplemented with  $8 \mu\text{g ml}^{-1}$  polybrene (Sigma-Aldrich).

## 2.3. Plasmids

The bacterial expression vector pET28 containing DNA constructs encoding either  $^{\text{a}}\text{RGD}$  or  $^{\text{a}}\text{RDG}$  has been described elsewhere [8]. pCMV-gag-pol and pCMV-VSVG were kindly provided by D.V. Schaffer (University of California, Berkeley). The human  $\alpha_5$ -GFP fusion construct was a gift from A.F. Horwitz (University of Virginia, Charlottesville) [14] and was subcloned from its original parent vector (pEGFP-N3) into the 5' *Hind*III and 3' *Not*I sites of the retroviral vector pLPCX (Clontech, Palo Alto, CA) in a two-step serial ligation procedure. Restriction digest of p $\alpha_5$ -EGFP-N3 with *Hind*III and *Not*I produced two fragments (A and B), which together encode the human  $\alpha_5$ -GFP construct. Fragment B (~900 bp) contained the 3' region of the  $\alpha_5$  integrin subunit fused to GFP and was ligated into *Hind*III/*Not*I-digested pLPCX using T4 DNA ligase. This intermediate pLPCX vector was verified to contain Fragment B by restriction digest and was treated with endonuclease *Hind*III to produce a linear form that was ligated to Fragment A, yielding the final pLPCX- $\alpha_5$ -GFP vector. The final product was verified by DNA

sequencing (Sequence/Structure Analysis Facility, California Institute of Technology) with 5' and 3' LPCX primers (Clontech) and alignment with NIH Blast (<http://www.ncbi.nih.gov>) to the human gene *ITGA5* (Accession # NM002205).

## 2.4. Recombinant protein expression

$^{\text{a}}\text{RGD}$  and  $^{\text{a}}\text{RDG}$  were produced in bacterial hosts using established methods [15]. Briefly, a 200 ml of overnight culture was used to inoculate a large-scale culture in a 10 l Bioflow 3000 fermentor (New Brunswick Scientific, Edison, NJ). Terrific broth (TB) supplemented with  $25 \mu\text{g ml}^{-1}$  kanamycin (Sigma-Aldrich) and  $34 \mu\text{g ml}^{-1}$  chloramphenicol (Sigma-Aldrich) was used as expression medium. The pH was maintained at 7.2, the temperature at  $37^\circ\text{C}$  and the dissolved oxygen concentration above 10% of air saturation. The culture was induced at an optical density at 600 nm ( $\text{OD}_{600}$ ) of 2–3 with 2.5 mM isopropyl-1- $\beta$ -D-thiogalactoside (IPTG) [Sigma-Aldrich], and expression was permitted to continue for 1.5 h until the  $\text{OD}_{600}$  reached a value of 10–12. The cells were harvested by centrifugation (15 min, 14,000 g,  $4^\circ\text{C}$ ) and each 10 l batch yielded an average of 200 g of wet cell mass.

## 2.5. Protein purification

Proteins were purified as described previously [15]. The wet cell mass was redispersed in TEN buffer (10 mM Tris-HCl, pH 8.0, 1 mM ethylene diamine tetraacetic acid (EDTA), 0.1 M NaCl) at  $0.5 \text{ g ml}^{-1}$  and stored at  $-20^\circ\text{C}$  overnight. The cells were defrosted at  $4^\circ\text{C}$  with  $10 \mu\text{g ml}^{-1}$  deoxyribonuclease 1 (Sigma-Aldrich),  $10 \mu\text{g ml}^{-1}$  ribonuclease A (Sigma-Aldrich) and  $50 \mu\text{g ml}^{-1}$  phenylmethylsulfonyl fluoride (Sigma-Aldrich) and then diluted in distilled water up to a final volume of 1.2 l. The solution was stirred at  $4^\circ\text{C}$  overnight, then brought to pH 9 using 6 N NaOH. After stirring for 1 h, precipitated impurities were removed by centrifugation (2 h, 28,000 g,  $4^\circ\text{C}$ ), and the supernatant was salinated to a NaCl concentration of 1 M. The supernatant was heated to  $37^\circ\text{C}$ , and the protein collected by centrifugation (2 h, 28,000 g,  $37^\circ\text{C}$ ). The resultant pellet was resuspended in  $4^\circ\text{C}$  distilled water at  $0.1 \text{ g ml}^{-1}$ . After repeating the process

twice, the final solution was dialyzed at 4 °C for 3 days, further purified through centrifugation (1 h, 38,000 g, 4 °C), frozen at –20 °C and lyophilized.

### 2.6. Fluorescence-activated cell sorting

CHO and CHO- $\alpha_5$  cells were suspended with 3 ml Versene (Invitrogen), centrifuged (3 min, 200 g) and resuspended in cold PBS. Analysis of GFP expression and cell sorting were performed using a FACSCalibur flow cytometer and a MoFlo cell sorter (DakoCytomation, Fort Collins, CO), respectively. Dead cells and debris were excluded according to their forward- and side-scatter properties. Analysis was performed with raw data transferred to Microsoft Excel.

### 2.7. Surface preparation

Corning tissue culture-treated polystyrene dishes were incubated overnight at 4 °C with 4 mg ml<sup>-1</sup> <sup>a</sup>RGD, 4 mg ml<sup>-1</sup> <sup>a</sup>RDG, 10 µg ml<sup>-1</sup> FN or 2 mg ml<sup>-1</sup> heat-inactivated (1 h, 55 °C) BSA (Sigma-Aldrich) in PBS. Prior to use, dishes were washed with cold PBS and blocked with 2 mg ml<sup>-1</sup> BSA in PBS at 37 °C for 1 h.

### 2.8. Spreading quantification

CHO and CHO- $\alpha_5$  cells were suspended using brief treatment with 1 ml trypsin–EDTA (0.05%, 53 mM). Suspended cells were immediately transferred to an equal volume of growth medium containing 1 µg ml<sup>-1</sup> soybean trypsin inhibitor (Sigma-Aldrich) and subjected to centrifugation (3 min, 175 g). Following two washes and resuspension in serum-free medium (CHO growth medium without FBS, supplemented with 1 mg ml<sup>-1</sup> BSA), 2.2 × 10<sup>5</sup> cells were seeded per 35-mm dish.

For antibody blocking studies, the BIIG2 antibody developed by Caroline Damsky was obtained from the Developmental Studies Hybridoma Bank at the University of Iowa. CHO- $\alpha_5$ -II cells were suspended to a final concentration of 10<sup>5</sup> cell ml<sup>-1</sup>, as described above. Cell suspensions were either left untreated or treated with BIIG2 antibody (1:40 final dilution) and were mixed for 30 min on a rotator at 4 °C before plating on protein-coated surfaces.

Cell spreading was followed by phase-contrast microscopy on an Axiovert 200M and image acquisition performed at four different locations with AxioCam MRm and AxioVision 3.1 software (Carl Zeiss MicroImaging, Thornwood, NY). The total number of cells and the number of well-spread cells were counted in each image to calculate the fraction of well-spread cells. For more objective characterization of cell spreading, cell areas were quantified using Scion Image (<http://www.scioncorp.com>). Histograms of cell area were generated and analyzed using Microsoft Excel (<http://www.microsoft.com>).

### 2.9. FAK phosphorylation

CHO and CHO- $\alpha_5$ -II cells were serum starved for 24 h and suspended using 1 ml trypsin–EDTA. Suspended cells were washed with soybean trypsin inhibitor and resuspended in serum-free medium. Cell suspensions were plated on 150-mm dishes coated with poly(2-hydroxyethyl methacrylate) (polyHEMA) and maintained on a rocker at 37 °C for 1 h to quiesce adhesion-dependent signals. Quiescent cells (1.5 × 10<sup>6</sup> cells) were plated on 60-mm dishes precoated with either <sup>a</sup>RGD or FN to initiate cell spreading. Meanwhile, a subset of quiescent cells were washed twice in ice-cold PBS and lysed in modified RIPA buffer (50 mM Tris–Cl (pH 7.5), 150 mM NaCl, 1% Triton ×–100, 0.5% NP-40, 0.25% sodium deoxycholate, 50 mM β-glycerophosphate (pH 7.3), 10 mM sodium pyrophosphate, 30 mM sodium fluoride, 1 mM benzamide, 2 mM EGTA, 1 mM sodium orthovanadate, 1 mM dithiothreitol, 5 µg ml<sup>-1</sup> aprotinin, 5 µg ml<sup>-1</sup> leupeptin, 1 µg ml<sup>-1</sup> pepstatin and 1 mM PMSF). After approximately 15 min at 4 °C, lysates were centrifuged at 14,000 rpm for 15 min, and the supernatant was collected. Micro-BCA protein determination (Pierce Biotechnology, Rockford, IL) was used to determine total protein concentration. Equal amounts of whole cell lysates were resolved by SDS–PAGE on 7.5% gels and blotted onto PVDF membranes (Bio-Rad Laboratories, Hercules, CA). Membranes were blocked overnight, then incubated with either anti-FAKpY397 antibody (BioSource International) or antiactin antibody (Santa Cruz Biotech), followed by incubation with corresponding HRP-conjugated secondary antibody (Pierce). Blots were treated with SuperSignal West Pico Substrate (Pierce)

and imaged on VersaDoc 3000 (Bio-Rad) using Quantity One software (Biorad).

### 3. Results and discussion

To determine whether  $^3\text{RGD}$  proteins support cell adhesion and spreading via the  $\alpha_5\beta_1$  integrin, we engineered cell lines that differentially express this integrin. CHO-B2 cells have been shown to express minimal levels of endogenous  $\alpha_5\beta_1$  integrin and  $\beta_3$  integrins [11–14]. These cells were infected with retrovirus encoding the human  $\alpha_5$  integrin subunit fused to GFP to generate the CHO- $\alpha_5$ -I cell line. The human  $\alpha_5$  integrin subunit effectively forms heterodimers with endogenous  $\beta_1$  integrin subunit in CHO cells, yielding  $\alpha_5\beta_1$  integrins whose function is not

perturbed by the C-terminal GFP fusion [14]. As a control, a separate pool of CHO-B2 cells (from hereon referred to as CHO) was infected with retrovirus generated using the corresponding empty vector (pLPCX).

This pair of cell lines was used to dissect the  $\alpha_5\beta_1$  integrin contribution to  $^3\text{RGD}$ -supported cell spreading. Both CHO and CHO- $\alpha_5$ -I cells were suspended and replated on tissue culture dishes preadsorbed with  $^3\text{RGD}$  (Fig. 1), a scrambled counterpart  $^3\text{RDG}$ , human plasma fibronectin (FN) or bovine serum albumin (BSA). After 3 h, CHO cells failed to spread on surfaces coated with either FN or  $^3\text{RGD}$  proteins (Fig. 2A). In contrast, CHO- $\alpha_5$ -I cells adhered and spread on both surfaces, demonstrating that the introduction of  $\alpha_5\beta_1$  integrin enables cell interaction with RGD-based aECM proteins. Furthermore,  $\alpha_5\beta_1$  integrin-

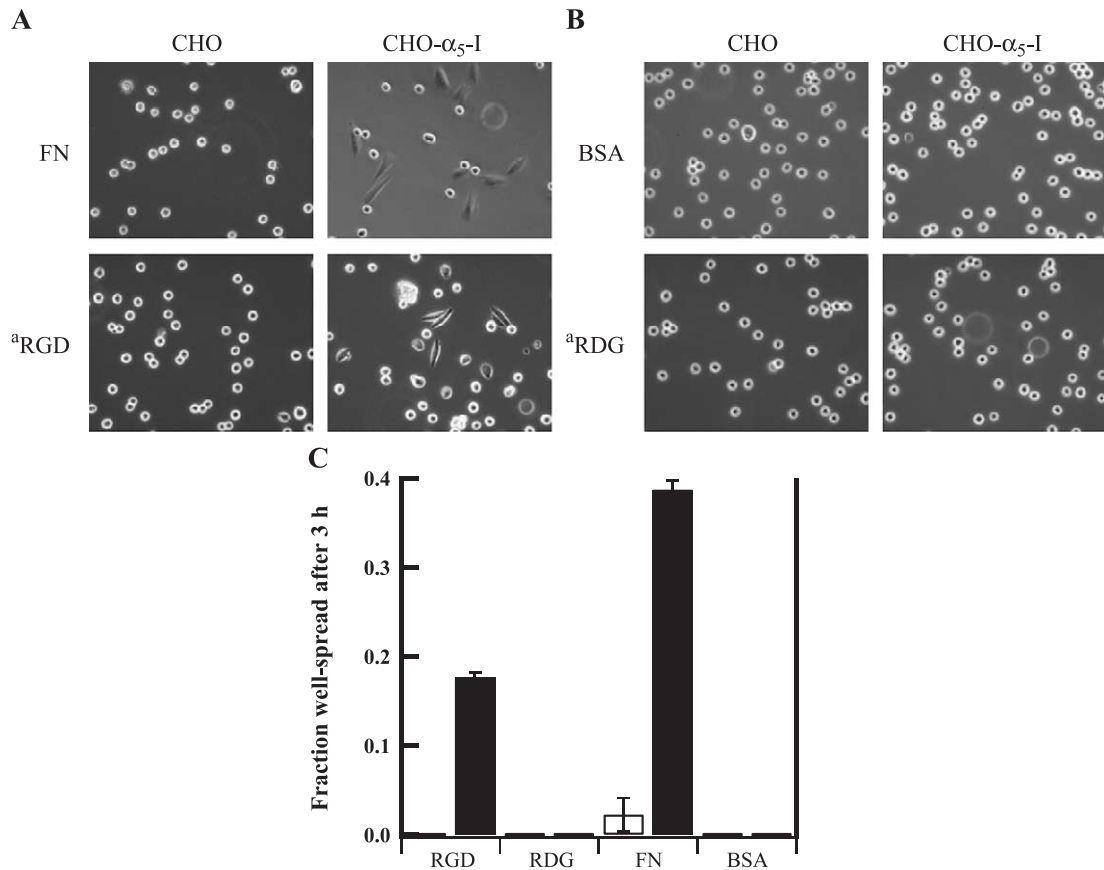


Fig. 2. Cell spreading on surface-adsorbed proteins. CHO and CHO- $\alpha_5$ -I cells were seeded on surfaces coated with (A) FN,  $^3\text{RGD}$ , (B) BSA or  $^3\text{RDG}$  for 3 h. A representative set of phase-contrast images is shown. (C) The fraction of CHO (empty bars) and CHO- $\alpha_5$ -I (filled bars) cells that were well-spread was quantified from images collected over 16 fields from four independent trials.

mediated cell spreading is specific to RGD-containing ligands since neither  $^a$ RDG- nor BSA-coated surfaces supported the spreading of either CHO or CHO- $\alpha_5$ -I cells (Fig. 2B).

To quantify these observations, the fraction of well-spread cells on each surface was determined by subjectively scoring cells from various fields into two categories: spread or not. As shown in Fig. 2C, while CHO cells lacking  $\alpha_5\beta_1$  integrin failed to spread on these surfaces, approximately 18% and 39% of CHO- $\alpha_5$ -I cells were well spread on  $^a$ RGD- and FN-coated surfaces, respectively. This data corroborates qualitative observations and establishes that the  $^a$ RGD protein supports  $\alpha_5\beta_1$  integrin-mediated adhesion.

CHO- $\alpha_5$ -I cell spreading mediated by FN is more extensive than that supported by  $^a$ RGD-coated substratum (Fig. 2A). This discrepancy may in turn affect scoring well-spread versus non-spread cells, especially in the case of CHO- $\alpha_5$ -I cells adhered to

adsorbed  $^a$ RGD, where the difference between spread and non-spread cells is not qualitatively striking. To obtain a more objective assessment of spread versus nonspread cells, we quantified projected cell area, regardless of spread phenotype. From this data, population distributions of cell area were calculated for both cell lines on various substrata (Fig. 3).

The distribution of cell area was unimodal for CHO cells exposed to any of the substrata, with a mean area of 165–186  $\mu\text{m}^2$  (Fig. 3A). Thus, a peak at approximately 180  $\mu\text{m}^2$  in the cell area distribution corresponds to the non-spread phenotype. In contrast to the unimodal distributions characteristic of non-spread cells, the area distribution for CHO- $\alpha_5$ -I cells on  $^a$ RGD- or FN-coated substrata had two components (Fig. 3B). While a low-area region of the distribution corresponded to the fraction of cells that were not spread, a second section of the distribution extended to areas greater than 290  $\mu\text{m}^2$ , corresponding

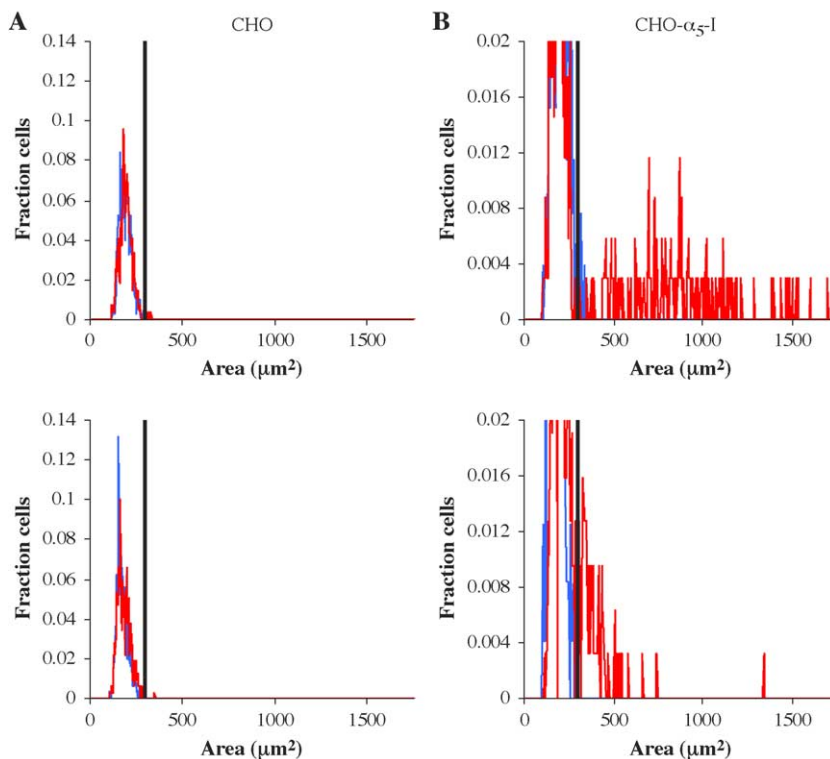


Fig. 3. Distributions of cell area among (A) CHO and (B) CHO- $\alpha_5$ -I cell populations after 3 h of exposure to protein-coated substrata. For each cell population, the spread areas of individual cells were quantified from images of approximately 300 cells gathered from three independent trials. A histogram of spread area is depicted for cells seeded on surfaces prepared with FN (red, top), BSA (blue, top),  $^a$ RGD (red, bottom) and  $^a$ RDG (blue, bottom). The black vertical line indicates the objective cut-off cell area of 290  $\mu\text{m}^2$  that demarcates non-spread from spread cells.

to the spread phenotype. Notably, the areas of spread cells on <sup>3</sup>RGD-coated surfaces were fairly close to the first peak, demonstrating in quantitative terms that distinguishing spread versus non-spread CHO- $\alpha_5$ -I cells may require a more rigorous approach.

To define objectively the range of cell areas corresponding to rounded cells, we used the spread-area distributions of CHO and CHO- $\alpha_5$ -I cells plated on BSA- or <sup>3</sup>RGD-coated surfaces. Approximating these histograms as normal distributions, we determined that a “cut-off” cell area of 290  $\mu\text{m}^2$  defines the low-area peak so that it includes 99.7% of rounded cells. Using the designated cut-off, the fraction of CHO- $\alpha_5$ -I cells that were spread on adsorbed <sup>3</sup>RGD was quantified to be 0.255 (Table 1), a value that is 42% higher than that approximated by subjectively counting well-spread cells (Fig. 2). Meanwhile, in the case of FN, the spread-cell fraction was 0.343, more closely matching the value estimated by the subjective method. Taken together, this data demonstrates that in the case where spread cells are clearly distinguishable from the non-spread phenotype, subjective counting may yield accurate results; however, in cases where spreading is limited, a more rigorous approach based on cell area distributions may be essential to quantify the fraction of cells responsive to adhesive substrata.

To understand better why only a fraction of the CHO- $\alpha_5$ -I cell population was responsive to <sup>3</sup>RGD- and FN-coated substrata, we quantified the distribution of  $\alpha_5\beta_1$  integrin expression in the CHO- $\alpha_5$ -I cell population. Because the  $\alpha_5$  integrin subunit is fused to GFP, flow cytometry was used to quantify GFP expression, resulting in a histogram of  $\alpha_5\beta_1$  integrin expression in CHO- $\alpha_5$ -I cells. As shown in Fig. 4, the CHO- $\alpha_5$ -I cell population exhibits a bimodal distribution of GFP expression, with the first peak corresponding to background autofluorescence that was also evident in the negative-control CHO cell

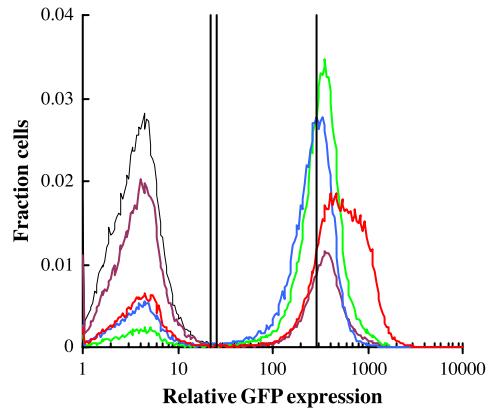


Fig. 4. FACS analysis of  $\alpha_5\beta_1$  integrin expression level. Fluorescence intensity (FI) of CHO (black), CHO- $\alpha_5$ -I (purple), -II (green), -III (blue) and -IV (red) cells were analyzed by FACS. A threshold FI of 22.3 (leftmost vertical line), below which autofluorescence of CHO cells was detected, helps to distinguish the nonexpressing and expressing cells. The middle vertical line defines the average threshold FI (26.0) required for spreading on FN-coated surfaces, while the rightmost vertical line defines a similar threshold FI (293) for spreading on <sup>3</sup>RGD-coated substrata.

population. The fraction of cells that expressed GFP-fused  $\alpha_5\beta_1$  integrin was 0.31, approximately matching the fraction of cells that spread on <sup>3</sup>RGD- and FN-coated substrata, establishing a quantitative correlation between  $\alpha_5\beta_1$  integrin expression and <sup>3</sup>RGD-supported cell spreading.

To corroborate this correlation, we determined whether enriching the cell population for  $\alpha_5\beta_1$  integrin expression would enhance the fraction of cells that spread on <sup>3</sup>RGD-coated substrata. The CHO- $\alpha_5$ -I cell population was enriched for GFP-expressing cells by fluorescence-activated cell sorting (FACS). As shown in Fig. 4, enrichment with different sorting criteria yielded three new cell populations (CHO- $\alpha_5$ -II, -III, -IV), each with a unique fraction of cells expressing  $\alpha_5\beta_1$  integrin (92.2%, 81.9% and 77.7%, respectively). As with CHO- $\alpha_5$ -I cells, sorted

Table 1  
Statistics of  $\alpha_5\beta_1$  integrin expression and spread areas for CHO and CHO- $\alpha_5$  cells

Cell population	Expressing $\alpha_5\beta_1$ integrin (%)	Relative $\alpha_5\beta_1$ integrin expression	Cells spread (%)		Mean spread area ( $\mu\text{m}^2$ )		Threshold level of $\alpha_5\beta_1$ integrin	
			<sup>3</sup> RGD	FN	<sup>3</sup> RGD	FN	<sup>3</sup> RGD	FN
CHO	0.338	n.a.	0.3	1.1	n.a.	n.a.	n.a.	n.a.
CHO- $\alpha_5$ -I	31.3	1.34	25.2	34.3	427	918	234	9.73
CHO- $\alpha_5$ -II	92.2	1.24	65.3	90.3	498	891	260	85.0
CHO- $\alpha_5$ -III	81.9	1	35.3	74.1	435	852	301	126
CHO- $\alpha_5$ -IV	7.7	2.12	51.1	87.4	477	840	402	4.40

CHO- $\alpha_5$  cells failed to spread on BSA- or  $^a$ RGD-coated surfaces, yielding histograms with mean cell areas of approximately  $160 \mu\text{m}^2$  (data not shown). From these histograms of non-spread cells, a cut-off cell area of approximately  $255 \mu\text{m}^2$  was identified to include 99.7% of cells. Applying this cut-off area to histograms of cell area for sorted CHO- $\alpha_5$  cells revealed that 90.3%, 74.1% and 87.4% of CHO- $\alpha_5$  -II, -III and -IV cells, respectively, spread on FN-coated surfaces, while 65.3%, 35.3% and 51.1%, respectively, spread on  $^a$ RGD-coated substrata (Table 1). Comparing the spreading behavior of sorted cells and that of unsorted CHO- $\alpha_5$ -I cells revealed that enriching for cells that express  $\alpha_5\beta_1$  integrin enhanced the fraction of cells that spread on  $^a$ RGD- and FN-coated substrata.

Interestingly, while the fraction of cells that spread on FN is significantly improved by enriching for cells that express  $\alpha_5\beta_1$  adhesion receptor, spreading on  $^a$ RGD-coated substrata is not comparably enhanced. This disparity is most evident in the CHO- $\alpha_5$ -III cell population wherein 74.1% of cells spread on FN, but only 35.3% spread on  $^a$ RGD. Despite this quantitative discrepancy in  $\alpha_5\beta_1$  integrin expression and cell spreading, the  $\alpha_5\beta_1$  integrin is mechanistically involved in cell spreading supported by both the natural and the artificial matrix proteins. Thus,

pretreatment with an antibody that has been shown previously to block  $\alpha_5\beta_1$  integrin-mediated adhesion of rat synovial fibroblasts [16] also inhibited CHO- $\alpha_5$ -II cell spreading on both FN- and  $^a$ RGD-coated surfaces (Fig. 5).

While these findings clearly implicate a common mechanistic dependence on the  $\alpha_5\beta_1$  integrin receptor, closer analysis of the histograms of cell spreading and integrin expression revealed quantitative disparities in how artificial and natural matrix proteins utilize the  $\alpha_5\beta_1$  integrin. Among the four cell populations expressing  $\alpha_5\beta_1$  integrin, the fraction of cells expressing the adhesion receptor closely matched the fraction of cells that spread on FN-coated substrata. Thus, simply imparting expression of  $\alpha_5\beta_1$  integrin is sufficient for spreading on FN. However, on  $^a$ RGD-coated substrata, a significant fraction of cells that express  $\alpha_5\beta_1$  integrin (approximately 18.5%, 29.2%, 56.8% and 34.3% in CHO- $\alpha_5$ -I, -II, -III and -IV, respectively) failed to spread, suggesting the hypothesis that spreading on  $^a$ RGD-coated substrata requires cells that not only express the adhesion receptor, but also express it at a level beyond a threshold requirement.

To test this hypothesis, an apparent threshold level of  $\alpha_5\beta_1$  integrin expression was determined independently for each  $\alpha_5\beta_1$  integrin-expressing cell line by calculating the critical fluorescence intensity (FI\*) at

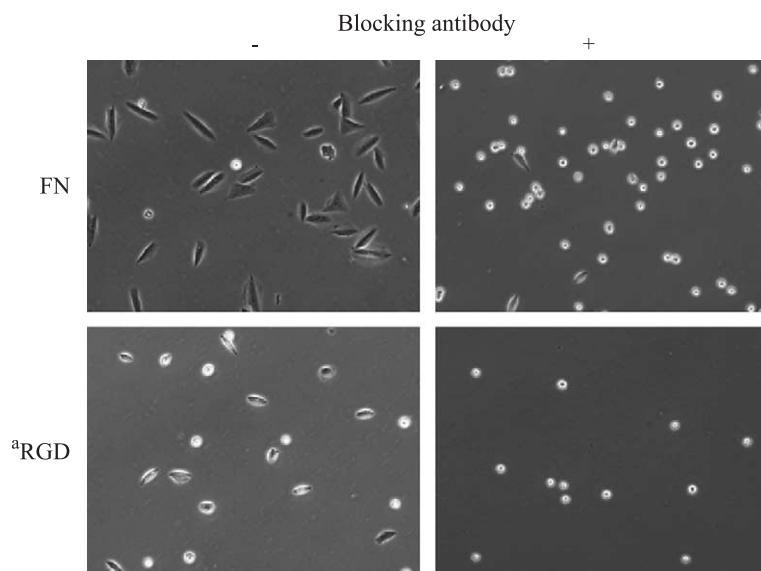


Fig. 5. Sensitivity of cell spreading to an  $\alpha_5\beta_1$  integrin-blocking antibody. CHO- $\alpha_5$ -II cells were seeded on FN (top panels) or  $^a$ RGD (bottom panels) either in the presence (right) or absence (left) of a blocking antibody BIIG2.

which the fraction of cells above FI\* equals the fraction of cells that spread on a particular substratum. As shown in Table 1, FN-coated surfaces required a mean threshold integrin expression level of 26.0. This threshold value closely matches the cut-off fluorescence intensity (22.3) segregating  $\alpha_5\beta_1$  integrin-expressing cells from those that do not express this receptor. This finding is consistent with the fact that expression of  $\alpha_5\beta_1$  integrin is sufficient for spreading on FN-coated surfaces, regardless of the level to which the adhesion receptor is expressed. Meanwhile,  $^a$ RGD-coated substrata required a mean threshold receptor expression level of 293, significantly greater than that required for spreading on FN. This order-of-magnitude discrepancy in the threshold amount of  $\alpha_5\beta_1$  integrin expression required for cell spreading helps to quantify the relative effectiveness of  $^a$ RGD and FN to support cell spreading using a common adhesion receptor.

Ultimately, the interest in  $^a$ RGD based or other biomaterials is not merely to promote cell spreading but also to initiate intracellular signals that elicit desired downstream cell responses. Among these integrin-mediated signals, focal adhesion kinase (FAK) phosphorylation is particularly important as it regulates cell survival, proliferation, migration and gene expression [17]. Moreover, it has been reported recently that phosphorylation of FAK on its Y397 residue requires the tethering of  $\alpha_5\beta_1$  integrin to the substratum [18]. Thus, other modes of stimulation, such as soluble-ligand binding and receptor clustering, fail to induce phosphorylation of FAK at Y397.

To test whether  $^a$ RGD-coated substrata support adequate integrin-mediated tethering, we gauged the ability of quiesced cells to phosphorylate FAK at

Y397 following 3 h of cell spreading on  $^a$ RGD- and FN-coated substrata. Cells were quiesced initially by withdrawing growth factor (serum-free medium) and by holding in suspension for 1 h. As shown in Fig. 6, these quiesced cells possessed minimal FAK phosphorylation at Y397. Upon seeding cells on  $^a$ RGD- or FN-coated surfaces for 3 h, FAK phosphorylation at Y397 was clearly detectable above initial basal levels, revealing that  $^a$ RGD supports adequate integrin tethering.

#### 4. Conclusion

Our analysis demonstrates that  $^a$ RGD-coated substrata support  $\alpha_5\beta_1$  integrin-mediated cell spreading, despite the absence of a PHSRN synergy site. Furthermore,  $\alpha_5\beta_1$ -mediated spreading on  $^a$ RGD-coated substrata elicits FAK signaling, an early integrin signaling event that regulates cell survival, proliferation, migration and gene expression. Taken together, these findings demonstrate that  $^a$ RGD supports both biophysical and biochemical functions, analogous to the roles played by natural extracellular matrix proteins.

Importantly, although both the artificial and natural ECM proteins are capable of utilizing the  $\alpha_5\beta_1$  integrin receptor, single-cell analysis of cell spreading and adhesion receptor expression revealed a significant quantitative difference. The threshold amount of  $\alpha_5\beta_1$  integrin receptor required for spreading on  $^a$ RGD-coated substrata was approximately 10-fold greater than that required for FN-mediated spreading. Indeed, this quantitative difference may be an underlying reason that  $\alpha_5\beta_1$  integrin-mediated cell spreading on  $^a$ RGD-coated substrata is masked in HUVEC, an endothelial cell line that spreads on  $^a$ RGD-coated surfaces using  $\alpha_v\beta_3$  integrin-enriched focal adhesions [8].

Taken together, these results emphasize the potential advantage of using complementary cell types to characterize the set of integrins that a biomaterial is competent to engage and the quantitative attributes of these interactions. In fact, such an approach may compensate for the fact that any ex vivo characterization, even with primary cells, is biased by a static snapshot of a cell population's adhesion receptor expression profile. In vivo, the functionality and

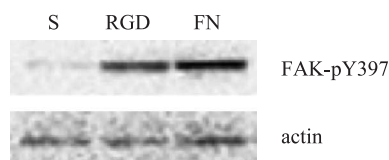


Fig. 6. Cell spreading-mediated FAK phosphorylation at Y397. The degree of FAK phosphorylation at Y397 (top panel) was probed by Western blotting lysates derived from quiesced CHO- $\alpha_5$ -II cells (lane 1) and quiesced CHO- $\alpha_5$ -II cells seeded for 3 h on surfaces coated with  $^a$ RGD (lane 2) or FN (lane 3). To verify that an equal amount of protein was present in each cell lysate, the level of actin was probed by Western blotting (bottom panel).

availability of endothelial cell adhesion receptors are modulated dynamically via changes in both expression level and affinity/avidity for its ligands [10]. Thus, the apparent flexibility of <sup>a</sup>RGD to mediate spreading via both  $\alpha_5\beta_1$  and  $\alpha_v\beta_3$  integrins may help to ensure that <sup>a</sup>RGD-based materials robustly maintain cell–material interactions in a wider range of in vivo contexts.

### Acknowledgements

The authors thank members of the A.R.A. and D.A.T. labs for helpful discussions and technical assistance. This work was funded by a start-up grant from California Institute of Technology to A.R.A. and NIH grant 5 R01 HL59987-03 to D.A.T. G.P.R. was partially funded by a graduate fellowship from the NSF-sponsored Materials Research Science and Engineering Center at California Institute of Technology.

### References

- [1] E. Danen, P. Sonneveld, A. Sonnenberg, K.M. Yamada, Dual stimulation of Ras/mitogen-activated protein kinase and RhoA by cell adhesion to fibronectin supports growth factor-stimulated cell cycle progression, *J. Cell Biol.* 151 (2000) 1413–1422.
- [2] S.J. Yarwood, J.R. Woodgett, Extracellular matrix composition determines the transcriptional response to epidermal growth factor receptor activation, *Proc. Natl. Acad. Sci. U. S. A.* 98 (2001) 4472–4477.
- [3] U. Hersel, C. Dahmen, H. Kessler, RGD modified polymers: biomaterials for stimulated cell adhesion and beyond, *Biomaterials* 24 (2003) 4385–4415.
- [4] E. Ruoslahti, RGD and other recognition sequences for integrins, *Annu. Rev. Cell Dev. Biol.* 12 (1996) 697–715.
- [5] S.D. Redick, D.L. Settles, G. Briscoe, H.P. Erickson, Defining fibronectin's cell adhesion synergy site by site-directed mutagenesis, *J. Cell Biol.* 149 (2000) 521–527.
- [6] S. Aota, M. Nomizu, K.M. Yamada, The short amino-acid-sequence Pro-His-Ser-Arg-Asn in human fibronectin enhances cell-adhesive function, *J. Biol. Chem.* 269 (1994) 24756–24761.
- [7] E.H.J. Danen, S.-I. Aota, A.A. van Kraats, K.M. Yamada, D.J. Ruiters, G.N.P. van Muijen, Requirement for the synergy site for cell adhesion to fibronectin depends on the activation state of integrin  $\alpha_5\beta_1$ , *J. Biol. Chem.* 270 (1995) 21612–21618.
- [8] J.C. Liu, S.C. Heilshorn, D.A. Tirrell, Comparative cell response to artificial extracellular matrix proteins containing the RGD and CS5 cell-binding domains, *Biomacromolecules* 5 (2004) 497–504.
- [9] A. Panitch, T. Yamaoka, M.J. Fournier, T.L. Mason, D.A. Tirrell, Design and biosynthesis of elastin-like artificial extracellular matrix proteins containing periodically spaced fibronectin CS5 domains, *Macromolecules* 32 (1999) 1701–1703.
- [10] P.E. Hughes, M. Pfaff, Integrin affinity modulation, *Trends Cell Biol.* 8 (1998) 359–364.
- [11] J. Ylanne, Y. Chen, T.E. O'Toole, J.C. Loftus, Y. Takada, M.H. Ginsberg, Distinct functions of integrin  $\alpha$  and  $\beta$  subunit cytoplasmic domains in cell spreading and formation of focal adhesions, *J. Cell Biol.* 122 (1993) 223–233.
- [12] C.L. Schreiner, J.S. Bauer, Y.N. Danilov, S. Hussein, M.M. Sczekan, R.L. Juliano, Isolation and characterization of Chinese hamster ovary cell variants deficient in the expression of fibronectin receptor, *J. Cell Biol.* 109 (1989) 3157–3167.
- [13] J. Takagi, T. Kamata, J. Meredith, W. Puzon-McLaughlin, Y. Takada, Changing ligand specificity of  $\alpha_v\beta_1$  and  $\alpha_v\beta_3$  integrins by swapping a short diverse sequence of the  $\beta$  subunit, *J. Biol. Chem.* 272 (1997) 19794–19800.
- [14] C.M. Laukaitis, D.J. Webb, K. Donais, A.F. Horwitz, Differential dynamics of  $\alpha_5$  integrin, paxillin, and  $\alpha$ -actinin during formation and disassembly of adhesions in migrating cells, *J. Cell Biol.* 153 (2001) 1427–1440.
- [15] S.C. Heilshorn, K.A. DiZio, E.R. Welsh, D.A. Tirrell, Endothelial cell adhesion to the fibronectin CS5 domain in artificial extracellular matrix proteins, *Biomaterials* 24 (2003) 4245–4252.
- [16] Z. Werb, P.M. Tremble, O. Behrendtsen, E. Crowley, C.H. Damsky, Signal transduction through the fibronectin receptor induces collagenase and stromelysin gene expression, *J. Cell Biol.* 109 (1989) 877–889.
- [17] S.K. Hanks, T.R. Polte, Signaling through focal adhesion kinase, *BioEssays* 19 (1997) 137–145.
- [18] Q. Shi, D. Boettiger, A novel mode for integrin-mediated signaling: tethering is required for phosphorylation of FAK Y397, *Mol. Biol. Cell* 14 (2003) 4306–4315.
- [19] E.R. Welsh, D.A. Tirrell, Engineering the extracellular matrix: a novel approach to polymeric biomaterials: I. Control of the physical properties of artificial protein matrices designed to support adhesion of vascular endothelial cells, *Biomacromolecules* 1 (2000) 23–30.
- [20] K. Di Zio, D.A. Tirrell, Mechanical properties of artificial protein matrices engineered for control of cell and tissue behavior, *Macromolecules* 36 (2003) 1553–1558.